Problems of Mathematical Modelling of Industrial Fixed-bed Reactors*

Gerhart Eigenberger and Wilhelm Ruppel**

Modelling and computer simulation for the purpose of design and operation of industrial fixed-bed reactors are discussed with the aid of examples. Emphasis is laid upon difficulties and problems arising from aiming at an adequate model formulation. The following aspects are discussed in some detail: 1) The influence of heat and mass transport in the catalyst pellet, especially with complex reactions. 2) Relationships between radial heat transfer and radial flow profile and its influence upon the temperature profile in packed tubes with or without heat generation by reaction. 3) Problems of adequate modelling of catalyst activity changes during the course of operation. 4) Scale-up problem of multitubular fixed-bed reactors, i.e. the problem of achieving and maintaining the same operating conditions in and around all the tubes of the bundle.

1. Introduction

Considerable progress has been achieved in recent years in mathematical description of the behaviour of fixed-bed reactors. The state of art is described in detail in textbooks [1-3] and review articles [4 – 6]. The object of this contribution is to point out a number of difficulties and problems arising when such mathematical models are used for calculation of industrial fixed-bed reactors.

In addition to the difficulties of a feasible description of the chemical reaction, which is referred to in [7], four different problem areas are usually encountered in practical work. These will be discussed in the following with the aid of examples. They are:

- the influence of heat and mass transport on the reaction in a catalyst pellet, especially with a complex reaction,
- the problem of heat and mass transport in packed tubes with exothermic chemical reaction, especially the influence of a radial flow profile,
- the problem of modelling changes in the activity of the catalyst during operation, and
- the scale-up problem for multitubular reactors, i.e. the question of how to ensure the same operating conditions over the whole cross-section of an industrial-scale reactor.

The discussion follows this list and leads from an individual catalyst pellet via packed single tube to multitubular reactor of industrial dimensions.

2. Influence of Heat and Mass Transport in the Individual Catalyst Pellet

The significance of the resistance to heat and mass transport between the gas and the catalyst surface and within the catalyst pellet to the conversion and selectivity of a heterogeneously catalyzed reaction has been known for a long time and is discussed in detail in the literature [1 – 3, 8]. In order to eliminate. distortion, due to transport effects, care is taken in the investigations of reaction kinetics, by ensuring suitable experimental conditions, that the rates of heat and mass transport are high, compared to the rate of reaction. There are a number of criteria given in literature for the estimation of this "kinetically controlled" experimental range (e.g. in [3], p. 190 ff.).

However, operating conditions for industrial fixed-bed reactors are often different. Due to pressure to produce higher conversions per catalyst volume, the developers of catalysts endeavour to make catalysts of higher activity with the result that most industrial catalysts are also used in the operating ranges in which the rate of reaction is high in comparison with the rates of mass and heat transport. In addition, industrial operation is characterized by high flow velocities in the packed bed, relatively large catalyst pellet diameters (3 to 10 mm) and relatively good thermal conductivity of the catalyst mass compared to that of the flowing gas. Under these

conditions, the constraints by pore diffusion and external heat transfer resistance are dominant in relation to the other transport resistances.

In spite of its great significance, the transport restriction in industrial catalysts was in the past normally taken into account only in the form of a constant correction factor, the so-called effectiveness factor. The following examples will show that this approach can lead to fundamental effects remaining unconsidered or being falsely interpreted. First, let us consider the synthesis of phosgene. In presence of active carbon, it occurs virtually without formation of any by-products, in accordance with Eq. (1):

$$Cl_2 + CO \rightleftarrows COCl_2 + 110 \ kJ/mol. \tag{1}$$

In practice, the strongly exothermic reaction is carried out in cooled multitubular reactors; it starts at temperatures below 100 °C; above 300 °C the reverse reaction (phosgene dissociation) increases in importance. Fig. 1a shows the calculation results for gas concentrations, temperature and rate of reaction plotted against the pellet radius for a single catalyst pellet in the main reaction zone. The calculation was carried out taking full account of multicomponent diffusion using the dusty-gas model [9], with the parameters given in Table 1. It can be seen that the composition of the flowing gas was selected to be almost stoichiometric. In spite of this, the ratio
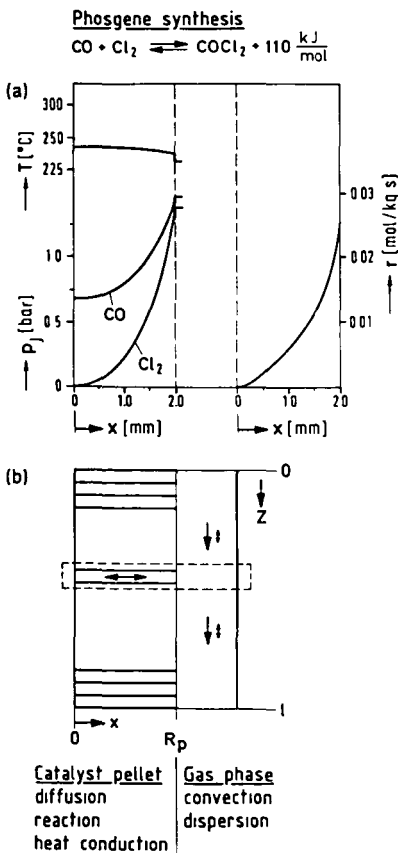

Phosgene synthesis

$$CO + Cl_2 \rightleftarrows COCl_2 + 110 \ \frac{kJ}{mol}$$

Fig. 1. a) Plots of temperature T, partial pressure p_j, and rate of reaction r against the pellet coordinate x for a single catalyst pellet in the main reaction zone; b) modelling and computation scheme of the heterogeneous plug flow model with reactor length as the z coordinate and the pellet coordinate x (R_p pellet radius).

Table 1. Model parameters for the calculated example of phosgene synthesis (Figs 1 and 2); R universal gas constant, M_j molar mass, k_p equilibrium constant, $k(T)$, $A(T)$ rate constants

Catalyst:	active carbon		
	single pellet diameter.	d_p =	4 mm
	mean pore radius:	r_p =	20 Å
	tortuosity factor	τ =	8
	porosity:	ε =	0.5
	thermal conductivity:	λ_p =	0.25 W/mK

Transport coefficients:

– Knudsen diffusion according to [3] $D_j^{Kn} = \frac{4}{3} r_p \sqrt{\frac{2}{\pi} \frac{RT}{M_j}}$

– binary diffusion coefficient according to Chapman, Enskog (compare [30])

– transport equation according to the dusty-gas model in the formulation by Jackson [9]

Kinetics (according to Shapatina et al:
Kinet. Catal. (USSR) 17 (1976) p. 559f)·

$$r \left[\frac{kmol}{kg\ s} \right] = k(T) \ \frac{P_{Cl_2} P_{CO} - \frac{1}{k_p} P_{COCl_2}}{(A(T) \ P_{CO} + P_{COCl_2})^{0.25} \left(\frac{A(T)}{k_p} + P_{Cl_2} \right)^{0.75}}$$

with $k(T)$ $= 10^{-7} \ e^{-4314/T}$

$A(T)$ $= 5 \times 10^{-3} e^{-4370/T}$

$\ln k_p$ $= -16.89 + 0.1337 \times 10^5 \ \frac{1}{T} + 0.3786 \times 10^{-3} \ T - 0.25 \times 10^{-7} \ T^2$

$(p_j$ in bar, T in K)

p_{CO}/p_{Cl_2} differs the more from 1, the deeper the penetration into the pellet. The reason for this is the severe restriction of the diffusion of the larger Cl_2 molecule, with the result that Cl_2 is removed by the reaction faster than it can be replaced by diffusion. In Fig. 1 this leads to the situation where, in the centre of the pellet ($x = 0$), Cl_2 disappears and the rate of reaction falls to zero.

The behaviour of an individual catalyst pellet is of less practical interest than that of the whole reactor. In the simplest form, the overall behaviour of the reactor, with the inclusion of the single pellet reaction, can be described by the so-called heterogeneous axial plug flow model (model B1 in the classification used by Froment [10] and Hofmann [4]). Fig. 1b shows the corresponding modelling and computation scheme. The model equation for convection transport in the gas phase is discretized along the reactor axis z, in the usual manner. The discretized gas phase balance equation is solved with that of the corresponding catalyst pellet at points along the axis.

If axial dispersion is disregarded then the overall behaviour of the reactor can be calculated in steps starting from $z = 0$. Fig. 2 shows the results of such a calculation for the synthesis of phosgene. The profile considered in Fig. 1 turns out to be a section of the complete computation at the position $z = 0.3$. The right-hand edges of the profiles in Fig. 2 indicate the conditions in the gas phase. The well-defined temperature maximum of the strongly exothermic reaction can be seen. In spite of this, the concentrations of the reactants decrease almost linearly, approximately as in the case of a zero order isothermal reaction. The reason for this is that there is a fairly large region within the catalyst pellet in which the rate of reaction disappears. This region can be subdivided into sections I to III. In
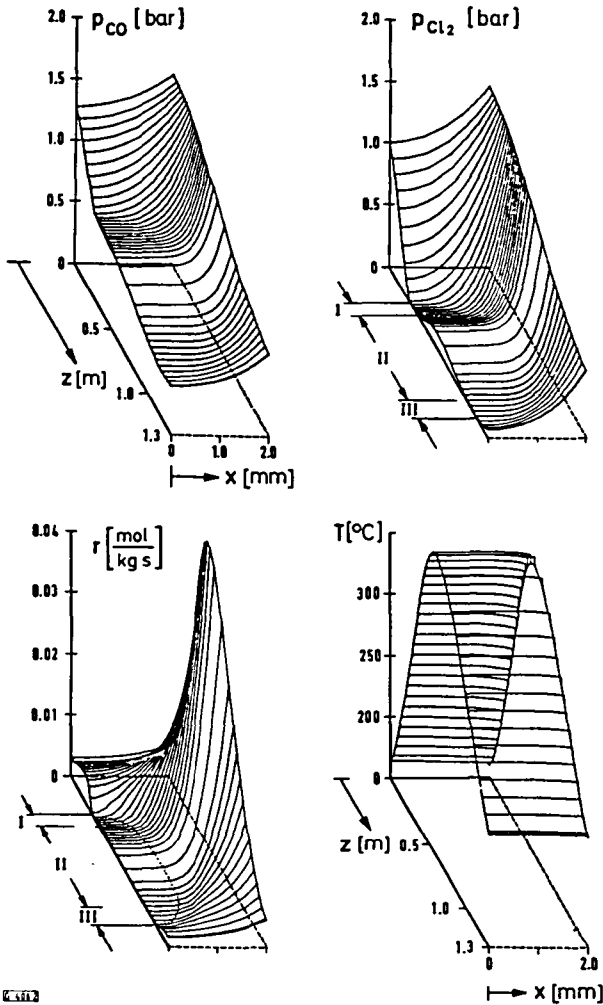
Fig. 2. Results of the heterogeneous plug flow model for phosgene synthesis.

$$PE \rightleftharpoons \begin{array}{l} \nearrow AC \\ \rightarrow AS \\ \searrow CO \end{array} \qquad (2)$$

In this way they succeeded in obtaining a good description of the reactor's behaviour over the whole range under investigation. An example of this is shown in Fig. 3a.

However, it must be pointed out that the quality of fit is no proof of the correctness of the reaction scheme (2). This assertion is illustrated by Fig. 3b in which the same measurements are matched with the following consecutive mechanism:

$$PE \longrightarrow AC \begin{array}{l} \nearrow AS \\ \searrow CO \end{array} \qquad (3)$$
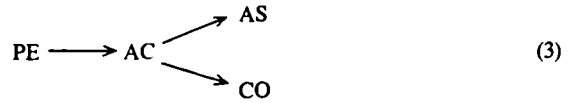
This had to be based, however, on a heterogeneous reactor model (type B1) instead of a pseudo-homogeneous model. Fig. 4 shows the complete calculation over the pellet radius and reactor length.

Fig. 3. a) Measurements of acrolein synthesis and model adaptation with a pseudo-homogeneous model and the parallel reaction mechanism (2) according to Arntz et al. [11]; b) calculation with a heterogeneous model and the consecutive mechanism (3); PE propene, AC acrolein, AS acrylic acid, $CO_x \equiv CO + CO_2$.
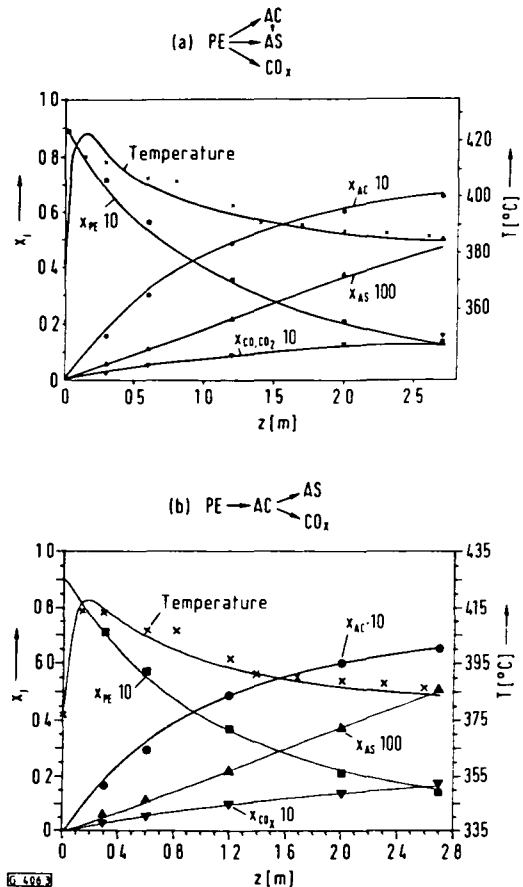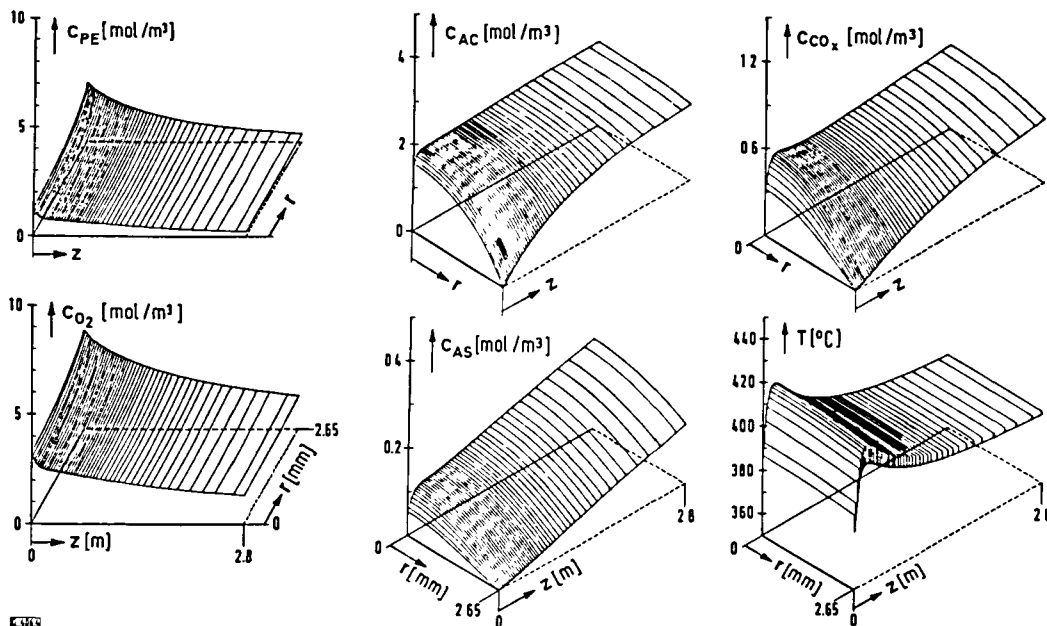
section I the rate of reaction is zero because, as discussed above, Cl_2 is completely consumed by the reaction. However, in section II, Cl_2 increases again, even in the centre of the pellet. The reason that, in spite of this, the rate of reaction remains at zero is that, with increasing temperature, the reverse reaction sets in and, hence, in the centre of the pellet the reaction is already at equilibrium. At the lower temperatures of section III, the conditions are the same as in I and, not until the temperature falls further, does the rate of reaction become so low that Cl_2 can diffuse into the centre of the pellet. It is clear that a (constant) effectiveness factor is not adequate for describing this "simple" reaction.

For the next example of a more complex reaction, let us consider the oxidation of propylene to acrolein. Arnzt et al. [11] investigated this reaction in detail under industrial operating conditions and described it by means of a pseudo-homogeneous plug flow model (model AIII in the classification of Froment [10] and Hofmann [4]). Since their measurements showed that both by-products, CO_x (CO and CO_2) and acrylic acid (AS), are formed along the reactor with finite initial gradient, they had to assume the following, purely parallel reaction mechanism (PE propene, AC acrolein):

Fig. 4. Concentration and temperature profiles versus reactor length z and catalyst pellet radius r for the model calculations as shown in Fig 3b.

It can be seen that with scheme (3) the acrolein formed in the interior of the first pellet reacts further to form CO_x and acrylic acid and for this reason both gas concentrations start along the z axis with finite initial gradient.

Reactions which, with pseudo-homogeneous description of the fixed-bed reactor, appear as parallel, can therefore in reality be a system of consecutive reactions. Here the concept of the simple pore effectiveness factor is overtaxed as it clearly cannot transform a parallel reaction into a consecutive one. In as far as the reactor model is only used for describing the behaviour of a given catalyst, the internal reaction mechanism is certainly of no consequence for practical application, provided that the measurable temperature and concentration behaviour patterns are satisfactorily reproduced. However, as soon as the model calculation is used to solve the problem of the catalyst's appropriate configuration, the internal mechanism becomes of decisive importance.

However, there is no wish to imply that the available models can be used for a "catalyst design" by computer. Neither the detailed understanding of various factors influencing the catalyst with respect to the course of the reaction on the (inner) surface nor the knowledge of the characteristic effects of pore texture on diffusion transport are sufficiently developed for this. Nevertheless, the model formulation is gaining in importance even for the questions of catalyst design, with regard to a qualitative and speculative preliminary formulation.

3. Influence of the Flow Profile in Catalyst-filled Tubes

Catalyst-filled tubes are characterized by point contact of the catalyst pellet at the tube wall and a definite mutual interlocking of the pellets in the interior of the bed (Fig. 5a). As a consequence, the void fraction (porosity) of the bed increases from a constant value in the interior (0.4 for spherical particles) to the value 1 at

the tube wall (Fig. 5b). Integral measurements in packed beds of spherical particles show a characteristic damped periodic porosity profile as illustrated in Fig. 5b. [12 – 15].

Corresponding to the larger free flow cross-sectional area, the mass flux (in kg/m²s) is larger in the vicinity of the wall than in the interior of the packed bed. This phenomenon, referred to as preferential peripheral flow, has been discussed in the past in conjunction with the question of radial geat transport in packed beds [16 – 19]. The present difficulty lies in the fact that so far no satisfactory measurement of the radial mass flux profile or of the equivalent superficial flow velocity has been obtained. (Measurements within the packed bed give considerably differing spot values, those above the bed are distorted by rapid radial equalization.)

A method of Vortmeyer and Schuster [12] has recently been used to calculate the superficial velocity profile from the porosity profile. The flow calculation is based on an Ergun equation for pressure drop in packed beds, extended to include wall effects. If the approximated porosity distribution, shown in Fig. 5b is assumed, this produces the radial flow profile illustrated in Fig. 5c (normalized with the mean void velocity $\bar{u}$). The preferential peripheral flow, according to Vortmeyer, is much more prominent than in the flow profile, according to Schwartz and Smith [18, 19], which is sometimes used (Fig. 6).

Fig. 7 shows the effect of the three different flow profiles shown in Fig. 6 on the calculation of a heating process (constant wall temperature and no reaction) in a tube containing a packed bed [20]. The calculation was carried out with a pseudo-homogeneous, locally two-dimensional model without axial conduction of heat (type AIII according to Froment [10] and Hofmann [4]). With the exception of the flow profile, all the model parameters are constant (Table 2); in particular, the same radial thermal conductivity was used throughout the calculation. Only the wall heat transfer coefficient α_w was adjusted in such a way that the same mean final temperature

Table 2. Model parameters for the calculated example shown in Figs 7 and 8b (according to [20]).

Model equations: Locally two-dimensional pseudo-homogeneous reactor model (type A III according to [4]) without axial diffusion/conduction of heat with radially variable flow profile as shown in Figs 6 or 8a.

Geometrical data:	Fig. 7	Fig. 8b
tube inner diameter [cm]	6.9	3.6
catalyst pellet diameter [mm]	10	5
tube length [m]	0.25	3.0

Physical properties:

− gas:		
density ρ_G [kg/m³]	1.11	1.17
specific heat capacity C_{pG} [kJ/kgK]	1.0	1.09
− packed bed:		
density [kg/m³]	1000	1000
effective radial thermal conductivity [W/mK]	0.335	0.824
effective radial diffusion coefficient [m²/s]	−	0.00032

Operating conditions:

mean cross-sectional loading G_z [kg/m²s]	0.167	1.0
wall or cooling temperature [°C]	100	300
inlet temperature [°C]	20	100
inlet concentrations C_A^0 [mol/m³]	−	5.5
C_B^0 [mol/m³]	−	22.2

Reaction parameters:

reaction scheme: A + B → C

rate of reaction $\left[\dfrac{\text{kmol}}{\text{kg s}} \right]$ $r = k(T)C_A C_B$
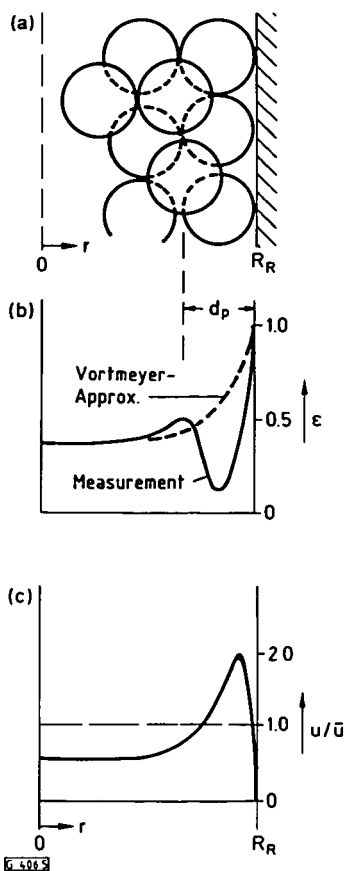
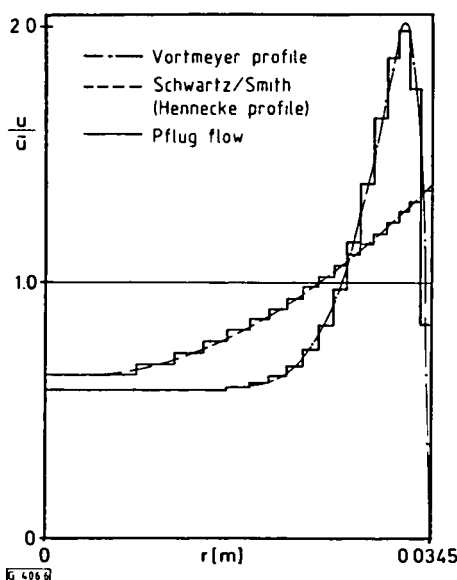with $k(T) = 10.7 \times 10^3 e^{-8000/T}$, T in K

$C_B = C_A^0 - (C_A^0 - C_A)$

heat of reaction $(-\Delta H_R)$: 150 kJ/mol

Fig. 5. a) Schematic representation of a packed bed of spherical catalyst pellets in a tube of radius R_R; b) measured and approximated porosity ε of a bed of spherical particles according to Vortmeyer and Schuster [12]; c) superficial velocity u profile calculated from the approximated porosity profile according to [12].

Fig. 6. Comparison of flow profiles according to Schwartz and Smith [18, 19] and Vortmeyer [12] with plug flow (pellet diameter d_p = 10 mm)

was achieved in every case. It can be seen that, under these conditions, there is a reasonable agreement between the profiles of the thermodynamic mean temperatures (however, the radial temperature profiles show larger differences, especially at the beginning of the packed bed). The fact that preferential peripheral flow requires the use of a distinctly smaller wall heat transfer coefficient than plug flow for the same degree of heating is explained by the main body of preferential peripheral flow being much closer to the wall.

Fig. 8 shows the effect on reactor calculations of using a preferential peripheral flow profile as opposed to plug flow [20]. A single exothermic reaction in a cooled reactor tube was considered with the reaction and physical properties, typical of industrial partial oxidation reactions (Table 2). Fig. 8a shows the basic geometry and the two flow profiles. Fig. 8b shows the axial temperature profiles and the radially averaged conversion plotted against the reactor length for the two types of flow. In the first part of the packed bed the cold reactor feed is heated through the wall and hardly any reaction takes place. Since, as in the previous example, the wall heat transfer coefficients were adjusted, the heating patterns of the two types of flow also agree with one another. However, substantial differences occur in the main reactor zone. There are two reasons
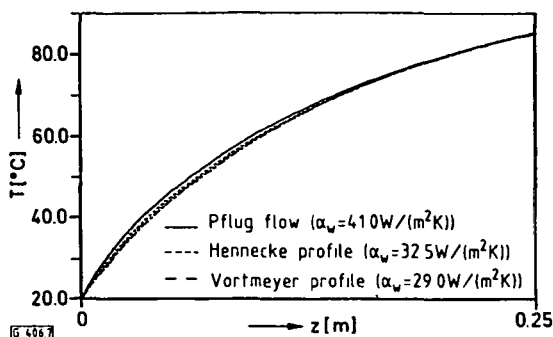
Fig. 7. Calculated profiles of thermodynamic mean temperature for a heating process at constant wall temperature T_W = 100 °C for the three flow profiles shown in Fig. 6. To obtain the same final temperature, the wall heat transfer coefficient α_W had to be adjusted as shown.

for this: with preferential peripheral flow the residence time on the axis of the tube is significantly longer than with plug flow. The reaction gas can therefore react further and release more heat. However, due to the lower wall heat transfer, this heat is not dissipated to the same extent as in the case of plug flow.

A similar difference in the calculated maximum temperature between plug flow and preferential peripheral flow has already been
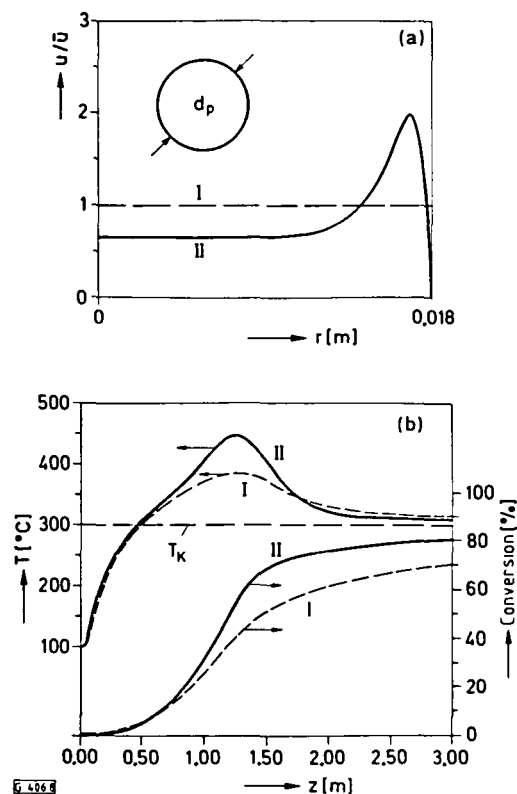

Fig. 8. a) Preferential peripheral and plug flow profiles for the following reactor calculation; b) axial temperature and conversion profiles of a simple exothermic reaction with plug flow (I) and preferential peripheral flow (II) according to [20]; T_K cooling temperature.

found by Lerou and Froment [21]. In contrast to the present calculation, these workers started from an empirical relationship for the flow profile (inversely proportional to the porosity profile) and from locally variable radial thermal conductivity.

Due to lack of reliable experiments, it is still an entirely open question as to which model representation is the most meaningful for heat transport in packed tubes with and without heat of reaction being released. The understanding of this problem is of great practical importance for the design and prediction of reactor behaviour for different catalyst and tube geometries.

In practice, the assumption of plug flow is usually maintained and at least one of the radial heat transport parameters is adjusted, e.g. the wall heat transfer coefficient α_W, together with the kinetic parameters. With exothermic reactions this produces values for α_W which can be more than double the values from the correlations of Hennecke [19] or Finlayson [29] (see also [4]).

With the joint adjustment of kinetic and heat transport parameters it is not possible to avoid mutual compensation for the model deficiencies (flow profile) by alteration of the kinetic parameters with the result that it is not safe to extrapolate a model, adjusted in this way, beyond the range of experimentation.

4. Changes of Catalyst Activity During the Operating Life of the Catalyst

It is well known that the behaviour of catalysts changes during their operating life. Usually, the catalyst becomes deactivated but occasionally an increase in activity is also observed. There is a large number of publications [22-24] on the causes of catalyst deactivation (sintering and recrystallization, poisoning and coking) and their modelling. However, in practice it is only rarely possible to determine and assign a clear cause. If, after a phase of initial activation or deactivation, the catalyst has a fairly long period of relatively constant activity, the kinetic model is related to this "run in" state. In cases in which the deactivation occurs progressively it must be considered in the model of the reaction. Fig. 9 shows the results of measurements for a partial oxidation reaction in which the deactivation produces a gradual retrograde displacement of the temperature maximum.

In model formulation it is usual to assume a separable deactivation, i.e. the rate of reaction is described by the product of a conventional reaction term $r(c,T)$, which is dependent on concentration and temperature and an activity a which varies with time and location:

$$r_{total} = a\,(z,t)\,r(c,t). \tag{4}$$

An activity balance must then contain the law governing the change of activity with time and location. In the present example it was obvious that the gradual retreat of the main reaction zone could be explained by a progressive loss of activity. The probable reasons were either a deterioration of the catalyst caused by the hot spot temperature, or catalyst poisoning caused by some unidentified trace material in the feed. The poisoning hypothesis proved to be the most suitable for describing the deactivation during the test. For four different times, Fig. 9 shows the measured temperature profile and the calculated temperature and relative activity profiles (actual activity based on the initial activity $a°$) including the actual operating conditions of the test which varied with time, over an operating period of 1000 h. The calculation was performed with a one-
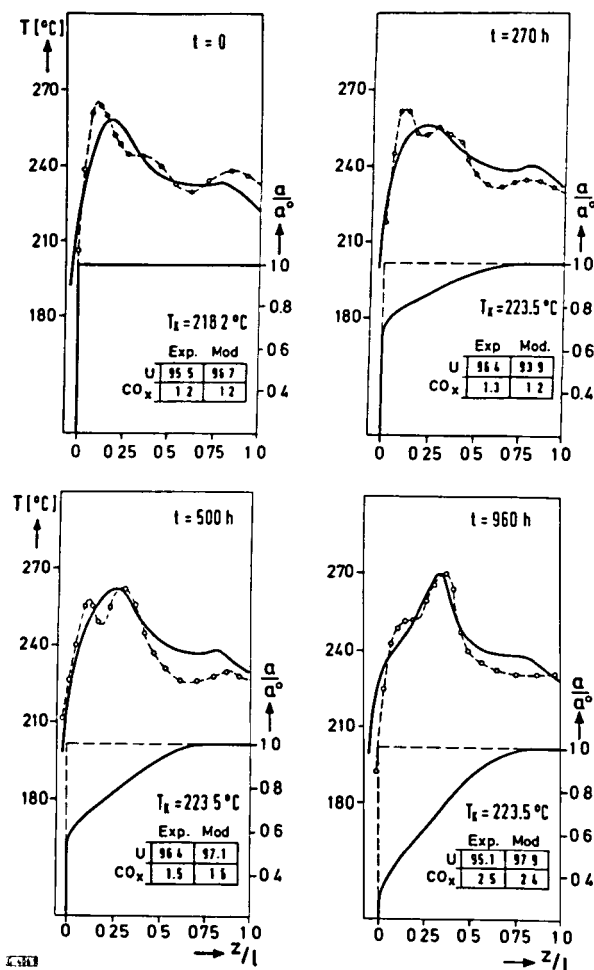
Fig. 9. Measured (points) and calculated (continuous line) temperature profiles and calculated activity behaviour at four different times for a partial oxidation reaction. In each case, the cooling temperature (T_K), conversion (U) and yield of by-products CO and CO_2 (COx) from experiment (Exp.) and model (Mod.) are plotted.

dimensional plug flow model which had been extended to include, in addition to the mass and energy balances, the following material balance for the catalyst poison and the activity balance:

$$u \; \frac{\partial y}{\partial z} \; = \; -a k_p y_p, \qquad (5)$$

$$C \; \frac{\partial a}{\partial t} \; = \; -a k_p \, y_p \qquad (6)$$

(u superficial velocity, y_p poison concentration based on value in feed).

The adjustment parameters for the deactivation behaviour were the capacity C of the catalyst for the contact poison and the rate constant k_p for poison chemisorption according to a first order reaction.

However, it is not often possible to describe the deactivation with reference to only one cause, as the following example will show. The purpose of the investigation was to develop a catalyst for an oligomerization reaction of hydrocarbons. One of the possible catalyst choices exhibited the deactivation behaviour shown in Fig.
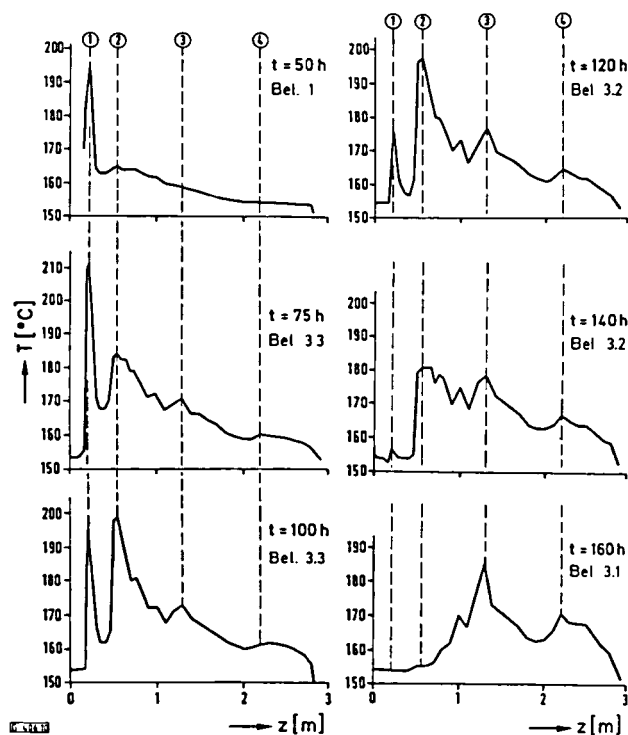

Fig. 10. Development of temperature profile for a hydrocarbon oligomerization reaction during the operating period t (constant operating conditions with the exception of throughput (Bel.)).

10. In spite of constant operating conditions and of uniform cooling temperature and catalyst quality along the reactor, temperature maxima occurred successively at four definite points, so that the main reaction zone was displaced ever deeper into the reactor. It is to be assumed that this deactivation is caused by at least two different mechanisms. The first one is a progressive deactivation which starts from the beginning with an effect similar to the earlier discussed poisoning. The second mechanism is evidently connected with the preceding temperature maximum. Presumably, in additon to the required products, long hydrocarbon chains are formed at the temperature maxima, which condense on the catalyst at lower temperatures and block the pores ("coking"). Without the first mechanism, this would produce an increasingly deep "hole" of coked catalyst after the first temperature maximum. However, the progressive deactivation causes the first temperature maximum to collapse after which the process is repeated deeper in the packed bed.

This type of deactivation process has so far eluded a quantitative model formulation. However, even in cases where the activity remains virtually constant over a long period, there is the question of whether the usual assumption of a constant activity from beginning to end of the reactor is justifiable. This applies, for instance, to partial oxidation reactions in which the degree of oxidation with high oxygen content at the reactor inlet is very different from that at the reactor outlet where the oxygen has been largely consumed [25].

5. Scale-up of Multitubular Reactors

The previous considerations applied to the reaction in a single tube. They have shown that the frequently used locally one-dimensional

plug flow model can reproduce the behaviour of the reactor under the test conditions only after comprehensive adaptation. This raises the question of whether it is really useful for scale-up calculations. On the other hand, the scale-up of multitubular reactors is supposed to be straightforward especially, as in the past, it was carried out without computer simulation. The only requirement was that, in the case of a multitubular reactor, the same optimum operating conditions should prevail in all the tubes as in the reference tube of identical dimensions, tested in the laboratory or pilot plant. However, behind the "only", there are sometimes concealed considerable practical difficulties. In this context it is necessary to differentiate between the operating conditions surrounding the tube and those inside the tube.

5.1. Operating Conditions around the Tubes

The ambient conditions for the tubes are chiefly related to the flow control of the heat transfer medium. McGreavy and Dunbobbin have discussed simple examples which show the additional effects occuring in presence of exothermic reactions if, during its passage through the tube bundle, the cooling medium is appreciably heated [26, 27]. For this reason, in strongly exothermic reactions (especially partial oxidation reactions) great emphasis is laid upon very small temperature differences between the cooling medium inlet and outlet. ΔT_k values of only a few degrees are demanded from and guaranteed by the equipment manufacturers either by circulating large quantities of liquid coolants or by evaporative cooling. However, conditions for endothermic cracking and fission are different from those for strongly exothermic reactions. In this case, flue gas (usually in a circulating gas distribution system) is normally employed as the heating medium. On account of the specific heat capacity being 1000 times lower, a considerable change in the temperature of the heating gas is unavoidable. Experience shows that, in practice, not always enough attention is being paid to the technological consequences of changing the heating gas temperatures.

As an example, let us consider a circulating flue-gas reactor of the design shown in Fig. 11. The flow of hot circulating gas in this instance is cross- and countercurrent to that of the reaction gas; the flow path is first directed radially inwards and, after turning, radially outwards.

If it is assumed that a single tube model exists which is adapted to the temperature range required here, then an overall model for the
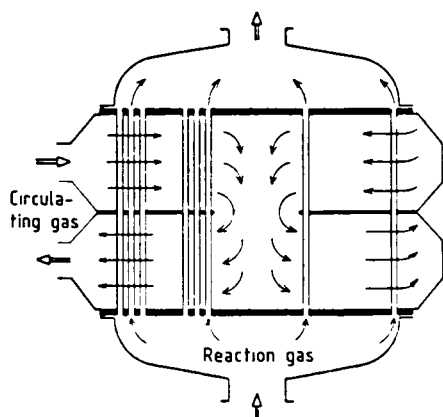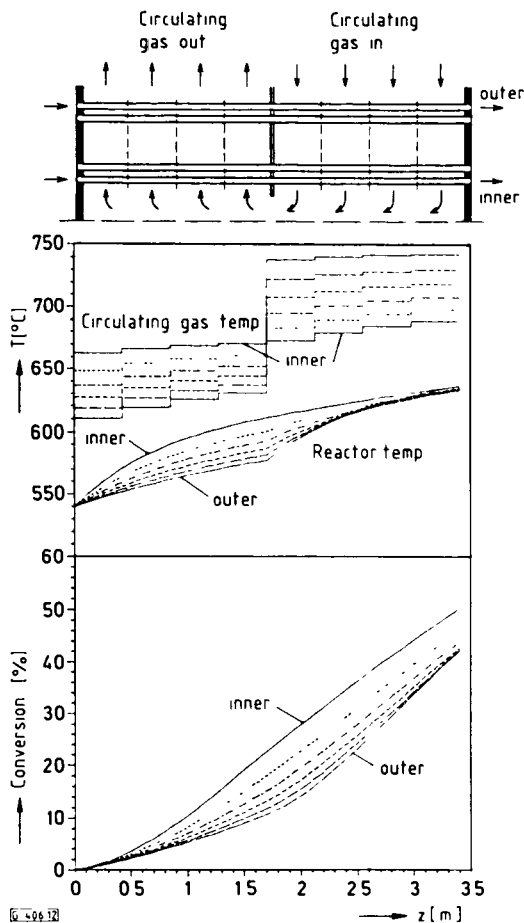

Fig. 12. Calculated circulating gas temperature, reactor temperature and conversion profiles for the multitubular reactor shown in Fig. 11

multitubular reactor can be formulated on this basis. In the following example, the circulating gas cycle is divided into 8 axial and 6 radial cells; for each cell, the circulating gas velocity and the resulting heat transfer coefficient are determined at the start of the calculation. Circulating gas temperature, and temperature and concentration profiles in the representative reactor tubes are computed jointly in an iterative process.

Fig. 12 shows the result of the simulation calculation for an actual application. The circulating gas enters the tube bundle at 750 °C. In the first radial elements, the temperature is reduced to between 740 and 735 °C by heat exchange with the outer tubes (the steps in the temperature profile are a consequence of dividing the system axially into discrete sections). The fall in temperature proceeds in the manner shown, with the assumption of complete mixing (temperature equalization) of the circulating gas at the point where the gas reverses its direction. The average outlet temperature is roughly 130 °C below the inlet temperature. The temperature and conversion profiles in the representative reactor tubes, as shown in the diagram, result from the interaction with the circulating gas temperatures. It is surprising that, in spite of the very different circulating gas temperatures, the final temperatures in all the tubes are almost the same. The reactor is therefore well designed as a heat exchanger. However, the differing temperature profiles in the individual tubes give rise to significant differences in conversion between the inner and the outer rows of tubes. In complex reactions

Fig. 11. Diagram of a reactor for endothermic reactions heated by circulating flue gas.

the spectrum of by-products will also be very diverse due to the differing temperature and conversion profiles, with the result that the concept of the reactor must be classified as unacceptable from the process engineering point of view. However, by varying the model, indications are easily found as to how the design could be improved. The influence of the operating conditions around the tubes on the behaviour of the reactor can therefore be assessed by model calculations based on simple single tube models which are correctly adapted for the desired range of operation.

5.2. Operating Conditions inside the Tube

The requirement of uniform operating conditions in the tubes which are maintained throughout the operating period is sometimes harder to fulfil. The prerequisite for this is that the reaction gas should enter all the tubes at the same temperature and concentration, which demands a carefully designed gas mixing section in the feed pipe. It is also necessary for each tube to have the same quality of catalyst and the same throughput. This is the more important the greater the sensitivity of the reaction to the parameters in the selected operating range. Here, again, partial oxidation reactions set very high requirements.

Equal throughput in all the tubes occurs if the flow conditions over the cross-sections of the hoods are equal and the pressure drops in the packed tubes are the same. Since the flow resistances in the hood are usually negligible in comparison to the pressure drop in the packed bed, the latter is of greater importance. With appropriate care and reproducibility during the filling of the tubes, the differences in pressure drop can be kept low. In spite of this, it does happen that an originally carefully filled reactor develops serious differences in pressure drop at the end of the operating period. Fig. 13 shows an example of this.
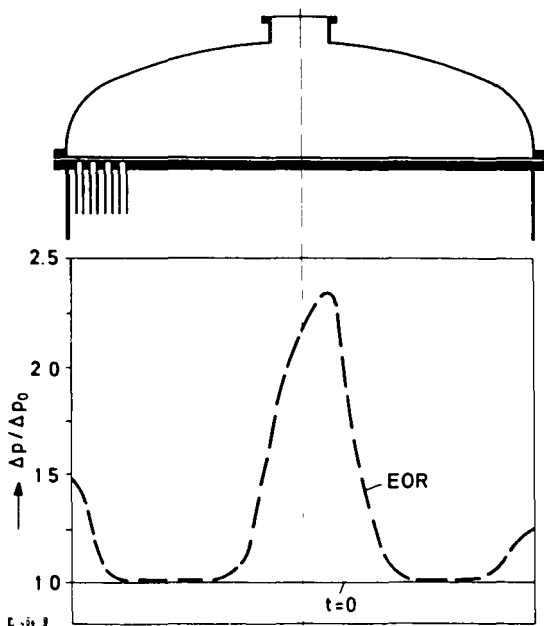
How the resulting progressive differences in throughput can affect the behaviour of the reactor is shown in Fig. 14 in model calculations for ethylene oxide synthesis by Westerterp and Ptasinsky [28]. According to this diagram halving of the throughput under otherwise unaltered conditions leads to a runaway reaction. This is because the heat transfer coefficient at the tube wall decreases with falling throughput. It is known that, in ethylene oxide reactors, the reaction in individual tubes or in sections of the tube bundle can apparently change spontaneously to total combustion.

With partial oxidation reactions in multitubular fixed-bed reactors, it is occasionally observed that the total combustion increases with increasing operating period. This forces a reduction in conversion or reactor loading and is frequently blamed entirely on catalyst deactivation. In the light of the processes discussed here, it could, however, also be a question of increasingly uneven distribution of the flow through the reactor.

6. Summary

The behaviour of multitubular fixed bed reactors is determined by

- the complex interaction of mass transport and reaction in the catalyst pellet,
- the interaction between flow, and generation and removal of heat in the catalyst-filled tube,
- the activation and deactivation behaviour in individual tubes,
- and the uniformity of the operating conditions inside and around the tubes.

In recent years considerable progress has been achieved in the formulation of models for these processes, with the result that it is now becoming increasingly possible to tackle practical problems in industrial reactors with the aid of computer simulation. Some examples of this have been discussed in the present contribution.
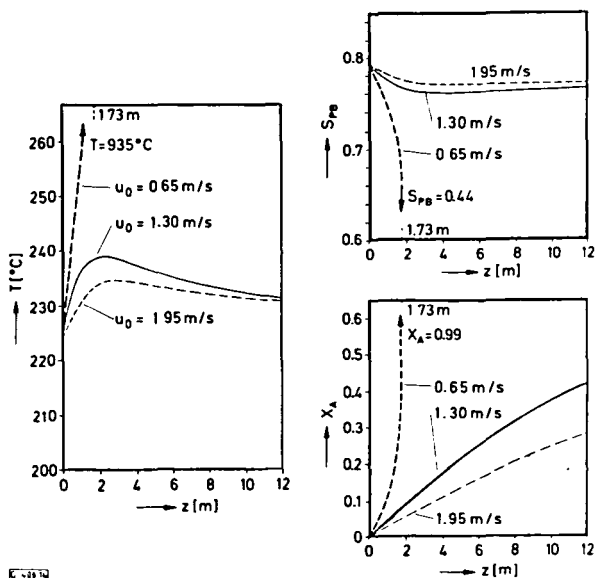

Fig. 13. Measured pressure drop profile over the cross-section of a multitubular reactor at the start ($t = 0$) and the end of the run (EOR).

Fig. 14. Influence of differences in throughput on the operating behaviour of a reactor tube in ethylene oxide sythesis (model formulation by Westerterp and Ptasinski [28]); T temperature, S_{PB} selectivity, X_A conversion.

At the same time, it had to be clearly pointed out that there are still a number of difficulties in modelling the processes referred to, which make the uncritical extrapolation of the model calculations rather risky. The authors hope that both, the possibilities and the problems indicated, will contribute to a realistic assessment of modelling as a tool in chemical reaction engineering.

References

[1] Smith, J.M., *"Chemical Engineering Kinetics"*, 3rd. Ed. McGraw-Hill Inc., New York 1981.

[2] Carberry, J.J., *"Chemical and Catalytic Reaction Engineering"*, McGraw-Hill Inc., New York 1976.

[3] Froment, G.F., Bischoff, K.B., *"Chemical Reactor Analysis and Design"*, John Wiley, New York 1979.

[4] Hofmann, H., *Ger. Chem. Eng* 2 (1979) No. 5, pp. 258 – 267.

[5] Deckwer, W.D., Serpemen, Y., *Fortschr. Verfahrenstech.* *16* (1978) pp. 275 – 296.

[6] Carberry, J.J., *Trans. Inst. Chem. Eng.* *59* (1981) pp. 75 – 82.

[7] Eigenberger, G., *Chem. Eng Process.* *18* (1984) pp. 55 – 65.

[8] Aris, R., *"The Mathematical Theory of Diffusion and Reaction in Permeable Catalysts"*, Vol. 1. Clarendon Press, Oxford 1975.

[9] Jackson, R., *"Transport in Porous Catalysts"*. Elsevier Scientific Publ. Co., New York 1977.

[10] Froment, G.F., *Proc. 5th Europ. Symp. Chem. React. Eng.*, Amsterdam 1972, A5-1.

[11] Arntz, D., Knapp, K., Prescher, G., Emig, G., Hofmann, H., *ACS Symp. Ser. 196* (1981) pp. 3 – 14.

[12] Vortmeyer, D., Schuster, J., *Chem. Eng Sci. 38* (1983) pp. 1691 – 1699.

[13] Benenati, R.F., Brosilow, C.B., *AIChE, J. 8* (1962) pp. 359 – 361.

[14] Goodling, J.S., Vachon, R.I., Stelpflug, W.S., Ying, S.J., Khader, M.S., *Powder Technol. 35* (1983) pp. 23 – 29.

[15] Schuster, J., Vortmeyer, D., *Chem.-Ing.-Tech. 52* (1980) pp. 848 – 849.

[16] Schertz, W.W., Bischoff, K.B., *AIChE J. 15* (1969) pp. 597 – 604.

[17] Calderbank, P.H., Pogorski, L.A., *Trans. Inst. Chem. Eng. 35* (1957) pp. 195 – 207.

[18] Schwartz, C.E., Smith. J.M., *Ind. Eng Chem. 45* (1953) pp. 1209 – 1218.

[19] Hennecke, F.-W., Schlünder, E.-U., *Chem.-Ing.-Tech. 45* (1973) pp. 277 – 284.

[20] Ufrecht, R., *Diplomarbeit*, Univ. Stuttgart 1983.

[21] Lerou, J.J., Froment, G.F., *Chem. Eng Sci. 32* (1977) pp. 853 – 861.

[22] Hughes, R., *"Deactivation of Catalysts"*, Academic Press. London 1984.

[23] Figueiredo, J.L. (Ed.), *"Progress in Catalyst Deactivation"*, NATO Adv. Study Inst. 1982.

[24] Delmon, B., Froment, G.F. (Eds.), *"Catalyst Deactivation"* (Proceedings Int. Symp., Antwerp 1980). Elsevier Publ. Co., Amsterdam 1980.

[25] Greger, M., Ihme, B., Kotter, M, Riekert, L., *Ber. Bunsenges Phys. Chem. 88* (1984) pp. 427 – 433.

[26] McGreavy, C., Dunbobbin, B.R., *4th Int. Symp. Chem. React. Eng,* III, pp. 96 – 106, DECHEMA, Frankfurt/M 1976

[27] McGreavy, C., Dunbobbin, B.R., *ACS Symp. Ser* (1978) No 65, pp. 214 – 224.

[28] Westerterp, K.R., Ptasinski, K.J., *Chem. Eng Sci. 39* (1984) pp. 245 – 252.

[29] Li, C.H., Finlayson, B.A., *Chem. Eng Sci. 32* (1977) pp. 1055 – 1066.

[30] Reid, R.C., Prausnitz, J.M., Sherwood. T.K., *"The Properties of Gases and Liquids"*, 3rd Ed., McGraw-Hill, New York 1977.